Autonomous Drone Measurement approach for Flying Base Stations

S. Tsakalidis[1], G. Tsoulos[1], G. Athanasiadou[1], V. Tsoulos [1]
[1] Wireless and Mobile Communications Lab, Department of Informatics and Telecommunications, University of Peloponnese, 22100 Tripolis, Greece, gtsoulos@uop.gr

***Abstract*— The widespread use of Unmanned Aerial Vehicles (UAVs) has been the key in expanding the application domain for antenna and field measurements. This paper proposes an original system for the measurement of the transmission patterns of flying basestations, using two drones. While one drone acts as a fixed radiation source with a transmitting antenna, the other conducts a survey over predefined trajectories to capture the received signal strength. The results from various flight plans—circular, cylindrical, and spherical—revealed consistent signal strength variations with max fluctuations of approximately 2.5 dB along the vertical axis, and the spherical flight providing comprehensive spatial coverage, all peaking towards the horizontal mounting pole of the transmit antenna. This work can serve as the basis for developing efficient UAV based measurement methods that will facilitate flying ad-hoc deployment and optimization of communication networks.**

***Index Terms*— UAV, flying base stations, measurement techniques, wireless communications.**

I. INTRODUCTION

In recent years, the rapid advancement of drone technology has paved the way for innovative applications across various domains. Among these, the concept of flying base stations with drones has emerged as a revolutionary approach to enhance wireless connectivity [1]–[4].

This novel solution leverages the mobility, flexibility, and rapid deployment capabilities of drones to provide temporary or supplementary network coverage in areas where traditional terrestrial infrastructure is insufficient, damaged, or non-existent. Flying base stations can be deployed in disaster-stricken regions to restore communication networks, in rural and remote areas to bridge the digital divide, and in densely populated urban centers to boost network capacity during large-scale events.

The integration of UAVs into antenna measurement systems provides a solution for the inefficiency and inaccuracy related difficulties. UAVs can navigate themselves to a specific location, fly complex flight paths and deliver surveying equipment to the centimetre [5]. This mobility allows for full 3-D mapping of radiation patterns, providing data in both near-field and far-field regions [6]. UAV-based measurements are easily performed in urban, rural, and remote environments, allowing for a more thorough characterization of the antenna performance across all environments [7].

In addition, the advent of the Internet Things (IoT) has led to even greater demands on wireless communication systems that need to be strong and resilient [8]. With the help of drones, measurements can be made in real-time, and network configurations can be adjusted automatically to maintain a high-quality connection service for IoT devices [9]. This is particularly useful in scenarios where traditional means of measuring are infeasible or impractical [10].

Nevertheless, to the best of the authors' knowledge, there is a gap in the literature regarding the measurement of real-world transmit patterns from a flying base station. Consequently, this paper presents a system where one drone, equipped with a transmitting antenna, acts as the fixed source, simulating the flying base station. Another drone, outfitted with measurement equipment, follows predefined trajectories to capture the power distribution around the transmitting drone. This method allows for the creation of a 3D map of the transmission behavior, which is crucial for understanding the performance in real-world operational scenarios.

This paper aims to achieve the following objectives:

1) Develop a Dual-Drone Measurement System: Design and implement a system where one drone simulates a flying base station and the other performs measurements.
2) Conduct Real-World Measurements: Employ UAVs for three-dimensional flights to capture actual signal responses, moving beyond theoretical analyses and simulations, to real-life data.
3) Validate Real-Time Data Collection: Demonstrate the capability of the system to perform real-time measurements and adjustments.
4) Optimize Network Performance: Use the real world measured data to suggest optimizations for wireless networks.

II. METHODOLOGY

A. Experimental Design

The design of the experiment concentrates on implementing a bi-drone system in order to measure the real-world transmitted pattern of flying Base Stations. It should be noted that the same methodology could also be applied to ground-based sites, where the flying Base Station would be substituted with a ground-based site.

The two drones were completely autonomous, using high-precision navigation and control systems for accurate flight path-following and coordination. The transmitting drone had a small but resourceful transmission system and hovered at a fixed location to simulate a flying base station. This transmission system also ensured minimal load on the drone, while providing a consistent signal for measurement. The measuring drone, equipped with an Single Board Computer (SBC) and software-defined radio (SDR), captured the transmitted data by following different flight patterns around the transmitting drone, to guarantee full spatial coverage. The experiment took place in a controlled outdoor area to reduce outside disturbance and to ensure data consistency. The location and time of the experiment were selected carefully to avoid any signal disruptions and offer a clear line of sight between the drones.

B. Data Collection

The primary data collected include:

- Signal Strength Measurements: The measuring drone captured the signal strength at various points in its flight path, recording the received signal strength indicator (RSSI) values.
- GPS Coordinates: GPS modules on the drones pro- vided precise latitude, longitude, and altitude data for each measurement point.
- Time Stamps: Each data point was time-stamped to ensure accurate synchronization between the drones and the measurement instruments.

The measuring drone executed different flight trajectories around the transmitting drone, maintaining a consistent distance from the transmitter to capture the radiation pattern in three dimensions. Throughout the flight, data were logged continuously in an onboard computer and real-time trans- mission of data to the ground station was achieved via the telemetry system of the drone. This dual approach allowed for storing data locally and immediate monitoring of the experiment's progress.

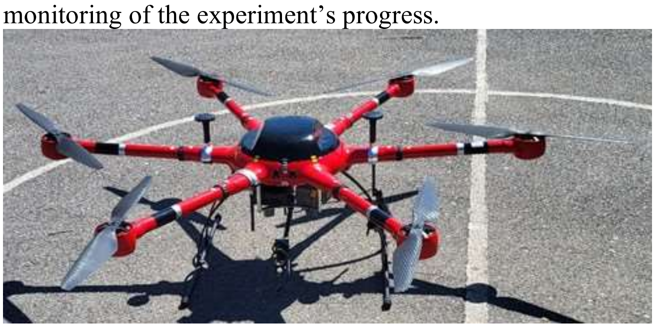

Figure 1. Haemus Hexacopter Skylle 1550 used in the experiments.

C. Data Analysis

The analysis of the collected data involved several steps to ensure accuracy and derive meaningful insights:

- Data Preprocessing: Raw data were first cleaned to re- move any anomalies or outliers, e.g. data points where GPS signals were weak.
- Coordinate Transformation: The GPS coordinates were transformed into a local coordinate system centered at the transmitting drone to facilitate easier analysis of the measurements.
- Interpolation and Smoothing: The discrete measurements were interpolated to create a continuous response.
- Visualization: The processed data were visualized using three-dimensional heat maps and contour plots, to illustrate the spatial signal strength distribution around the transmitting drone.

III. EXPERIMENTAL SETUP

The setup of this study required the use of both a transmitting and a measuring drone. This involved fine-tuning the drones, establishing data recording protocols, setting up the ground control station, adjusting for environmental conditions, and implementing calibration and validation procedures.

A. Drone Specifications

The drones deployed in the experiments were Haemus Hexacopter Skylle 1550 models (Fig. 1), selected for their endurance and payload capabilities. They offer a flight duration of up to 75 minutes and can transport payloads up to 10 kg. The drones are equipped with advanced navigation systems, feature autonomous take-off and landing, are stabilized by Cube Orange flight controllers, and include ADS-B receivers to enhance system stability and safety.

B. Transmitting Drone Configuration

For the transmitting drone, an Arduino microcontroller (MCU) with a 433 MHz transmitter was utilized. The transmission system operated at 433 MHz with a power output of 10 mW, transmitting a continuous wave (CW) signal. The Arduino, powered by a 5V supply, ensured a consistent signal for measurement purposes. To optimize the signal transmission, a custom-designed lightweight spring antenna was used. Made of copper-clad wire, the antenna is easy to solder and integrate into the system. It is compact, measuring approximately 38mm in length, with a gain of 2 dBi and an impedance of 50 Ohm.

Beneath the drone's body, a horizontal antenna mounting pole was affixed, extending predominantly in one direction but remaining within the drone's overall footprint. This specific configuration was chosen to clear the space in that direction around the drone, thereby simplifying the visualization of spatial measurements. The drone maintained a steady hover at an altitude of 50 meters above ground level, adhering to a predefined autonomous flight plan to ensure consistent stability and repeatability (Fig. 2). This height was chosen to optimize signal clarity while accommodating the practical requirements of drone stability under varying wind conditions.

C. Measuring Drone Configuration

The measuring drone was equipped with a Raspberry Pi 4 SBC and a Mini Digital USB 2.0 TV Receiver RTL-SDR with a 433 MHz, 2 dBi gain antenna. They stored captured radio signals on high-speed flash memory, filtered them with a low-pass filter on board, and measured every 0.1 seconds the power of these signals. We selected the Raspberry Pi 4 for its significantly enhanced processing power and its ability to interface with various sensors and peripherals. Among the additional equipment integrated was the TOPGNSS GN-803G, a USB GPS sensor that delivers precise location data for accurate geo- tagging of measurements. The GPS sensor was also used for precise timekeeping, allowing for the accurate synchronization of future measurements with different equipment.

Figure 2. The transmitting drone (top) and the measuring drone (bottom) in flight (as seen from the ground).

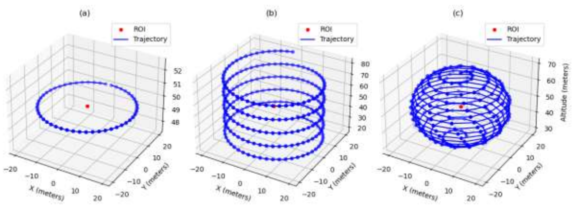

Figure 3. Flight patterns of the measuring drone: (a) Cyclical, (b) Cylindrical, (c) Spherical. ROI indicates regions of interest and represents the position in space of the transmitting drone.

D. Data Collection

The primary data types included signal strength measurements, GPS coordinates, and timestamps. The measuring drone followed various flight patterns, such as cyclical, cylindrical, and spherical trajectories, around the transmitting drone, with a fixed radius at 10m. These patterns were chosen to capture the signal distribution in three dimensions. The target point in space, where the transmitting drone was hovering, was always at the center of the measuring drone's trajectory. This setup ensured that the entire spatial domain around the transmitter was thoroughly scanned (see Fig. 3).

The altitude range was kept at a fixed 50 meters relative to the ground, chosen to minimize the effects of multipath reflections from the ground while ensuring stability against wind disturbances. Each flight session lasted between 5 to 10 minutes, allowing for comprehensive data collection within the battery constraints of the drones. Each flight was run at a controlled speed to ensure consistent data sampling rates, and each of the drones flew its own autonomous navigation plans to execute precise flight patterns.

A custom script written in Python to log the data was run as a Linux service on the Raspberry Pi 4. The script was designed to initiate data logging upon detecting a significant altitude change, preventing unnecessary data storage during the drone's ascent and descent. Each measurement iteration captured the GPS location, time, and SDR measurements, storing the data locally on an onboard SD card for redundancy. Simultaneously, real-time data transmission to the ground station was facilitated via the drones' telemetry systems, which utilized a robust communication protocol to handle the data rate and ensure error-checking.

Figure 4. The ground stations for the transmit and receive drones

E. Ground Station Setup

The ground station configuration was essential to monitoring and controlling the experimental run (Fig. 4). Mission Planner software was used for planning, configuring, simulating, and monitoring the autonomous missions. Mission Planner is a versatile ground control station (GCS) software that provides real-time telemetry, flight planning, and control capabilities. It is tailored to the needs of the experiment, monitoring all parts of the flight and data measurement. To make the job safer, the software included features such as geofencing, fail-safe protocols, and instant alerts in case of deviations from the pre-programmed flight path.

Real-time data reception and processing were facilitated through the drones' telemetry systems. Data was collected via TCP using the Python library pymavlink, which enabled seamless communication between the drone and the ground station. The ground station was equipped with high-gain antennas to ensure robust communication links, even over extended distances and in challenging environments. Backup telemetry links and data logging mechanisms were in place to ensure data loss would not occur nor would the system be inoperative. These measures ensured that the data integrity was maintained throughout the experiment and that any potential issues could be promptly addressed.

All the experiments were conducted in an open field near the Wireless and Mobile Communications Lab of the University of Peloponnese. The location was chosen for its open space, minimizing potential sources of signal reflection and obstruction. The measurements were performed in optimal weather conditions, specifically with limited wind, to ensure stability during flight. Throughout the study, environmental conditions were continuously monitored to maintain a consistent quality of the data set. All flights were conducted in accordance with European Union Aviation Safety Agency (EASA) regulations and were carried out by authorized personnel. Calibration of the measurement equipment was performed in the lab. Repeated calibration steps were conducted prior to each flight to allow for potential drifts in the performance of the equipment.

IV. Results and Discussion

This section presents the results obtained from the experimental flights, which involved different types of flight plans, data recorded on board and analysis of measurements collected from the UAVs.

A. *Evaluation of Position Accuracy*

The statistical assessment of positioning errors provides a quantitative evaluation of the deviations observed between the planned and actual trajectories of the measuring drone (at distance 20m). The assessment consists in computing positional errors along x, y and z-axes as well as the combined error, to provide a comprehensive understanding of the drone's positional accuracy. The probability density functions (PDFs) of the positioning error along x, y and z axes are presented as well as for the total errors in Fig. 5. These distributions are generated using kernel density estimation (KDE) to generate a smooth estimate of the error distributions.

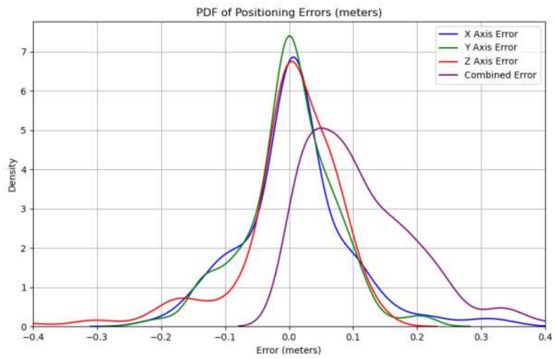

Figure 5. PDF of Positioning Errors (meters): KDE plots showing the error distributions along the x, y, and z axes, as well as the combined error.

X-Y Plane Errors: The mean error in the x-y plane is 0.09 meters, with a standard deviation of 0.07 meters and a maximum error of 0.36 meters.

Z Axis Error: The mean error along the z-axis is 0 meters, with a standard deviation of 0.09 meters and a maximum error of 0.15 meters. The small mean error suggests that the drone maintained a consistent altitude throughout the flight, with minimal vertical deviations.

Combined Error: The mean combined error, which takes into account deviations in all three dimensions, is 0.11 meters, with a standard deviation of 0.09 meters and a maximum error of 0.49 meters.

The low mean and standard deviation values indicate that the measuring drone's navigation system is precise, ensuring that the data collected is reliable and accurate. The low vertical errors observed support the reliability of the altitude control systems on the drone, important to keep measurement conditions consistent.

B. *Flight path Results*

The results of each experimental campaign were obtained with a set of carefully orchestrated flight missions that aimed at measuring the GPS coordinates, and timestamps, which together with the signal strength measurements form a detailed three-dimensional map of the transmitted signals in various directions.

1) Circular Flight Plan

This flight path was designed to capture the azimuthal variation in the signal strength. Fig. 6 gives an actual flight trajectory of the drone for the circular flight plan. The waypoints of this flight plan are indicated in Figure 3a and the path (color-coded based on the measured signal strength at each point) offers an intuition of how the signal varies around the transmitter. The signal strength varied consistently around the circular path within a window of 0.5 dB, which is expected due to the almost perfect line-of-sight conditions during these measurements. Also, it showed its peak towards the direction of the horizontal mounting pole used for the transmit antenna.

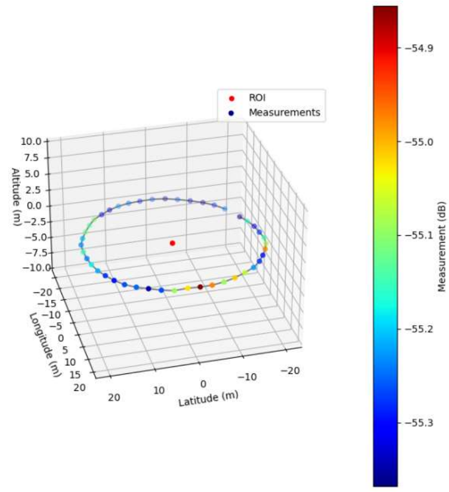

Figure 6. Circular flight plan: Actual trajectory of the measuring drone, with color-coded signal strength measurements.

2) Cylindrical Flight Plan

The cylindrical flight plan involved the measuring drone following a vertical cylindrical trajectory around the fixed position of the transmitting drone. The flight path was meant to sample the signal strength intensity for varying heights.

Fig. 7(a) shows the actual trajectory of the drone during the cylindrical flight plan along with the color coded measured received power. The waypoints of this flight plan are visualised in Figure 3(b). A smoothed, interpolated and continuous 3D mapped surface is shown in Figure 7(b).

The signal strength fluctuated ~2.5dB with respect to the vertical axis, with certain altitudes showing higher or lower values. As also for the circular case, it clearly showed its peak towards the direction of the horizontal mounting pole used for the transmit antenna.

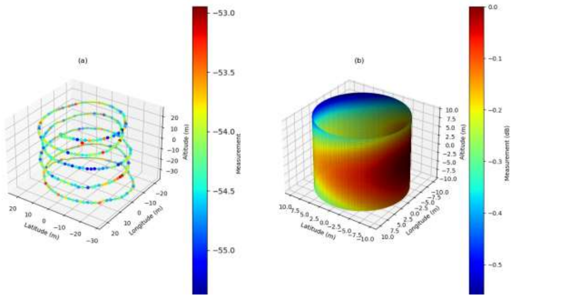

Figure 7. Cylindrical flight plan: (a) Actual flight trajectory of the measuring drone with color-coded signal strength measurements. (b) Interpolated 3D cylindrical surface.

3) Spherical Flight Plan

The spherical flight plan involved the measuring drone following a spherical trajectory around the fixed position of the transmitting drone, giving a complete spatial coverage of the signal strength. Fig. 8(a) illustrates the actual flight trajectory of the drone during the spherical flight plan along with the color coded measured received power. The waypoints of this flight plan are shown in Fig. 3(c). As also for the circular and cylindrical cases, it is now even more clear that the peak of the signal strength is towards the direction of the horizontal mounting pole used for the transmit antenna.

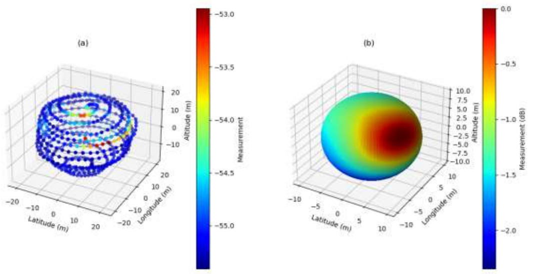

Figure 8. Spherical flight plan: (a) Actual flight trajectory of the measuring drone with color-coded signal strength measurements. (b) Interpolated 3D spherical surface.

The 3D plots clearly illustrate a symmetrical pattern in the measurements from north to south, influenced by the same factors in an interchangeable manner. In the north, the receiving drone's illumination zone is unobstructed, while the transmitting drone's is obstructed; conversely, in the south, the situation reverses, with the transmitting drone's zone clear and the receiving drone's obstructed. Generally, the impacts observed from the drone's body and particularly its carbon fiber propellers, as reported in existing literature, [11], align with the results found in this study.

V. Conclusions

This study has presented an evaluation of the performance and accuracy of a drone-based measurement system for mapping the transmission patterns of flying base stations. The experiments demonstrated good positional accuracy that indicates the precision and reliability of the drone's navigation system. The results from various flight plans revealed consistent patterns in signal strength variations. The spherical flight plan provided comprehensive spatial coverage, confirming that peak signal strength consistently aligned with the horizontal mounting pole direction. The 3D mapping of signal strength revealed symmetrical patterns influenced by the drone body and propeller materials, aligning with findings in existing literature. These patterns were particularly evident in the symmetrical influence observed from north to south, where obstructions alternated between the transmitting and receiving zones of the drones. These findings underscore the significant potential of drones in providing reliable data for mapping the transmission patterns of flying base stations, thus enhancing our understanding of wireless systems in real-world operational scenarios. The results of this study have also implications for field testing and validation of new antenna designs and deployments under real-world conditions.

Acknowledgments

This work is supported by the SYNERGIES project, funded by the European Commission Horizon Europe program, Grant Agreement No. 101069839.

References

[1] G. Amponis, T. Lagkas, M. Zevgara, G. Katsikas, T. Xirofotos, I.Moscholios, and P. Sarigiannidis, "Drones in b5g/6g networks as flying base stations," Drones, vol. 6, p. 39, 2 2022.

[2] A. Fotouhi, M. Ding, and M. Hassan, "Service on demand: Drone base stations cruising in the cellular network." IEEE, 12 2017, pp. 1–6.

[3] Z. Becvar, M. Vondra, P. Mach, J. Plachy, and D. Gesbert, "Performance of mobile networks with uavs: Can flying base stations substitute ultra-dense small cells?" IEEE, Ed., 2017, 2017 IEEE.

[4] G. E. Athanasiadou, M. C. Batistatos, D. A. Zarbouti, and G. V. Tsoulos, "Lte ground-to-air field measurements in the context of flying relays," IEEE Wireless Communications, vol. 26, pp. 12–17, 2 2019.

[5] Y. Zeng, R. Zhang, and T. J. Lim, "Wireless communications with unmanned aerial vehicles: opportunities and challenges," IEEE Communications Magazine, vol. 54, pp. 36–42, 5 2016.

[6] Q. Yuan, Y. Hu, C. Wang, and X. Ma, "3d beamforming for improving the security of uav-enabled mobile relaying system," Radioengineering, vol. 27, pp. 304–311, 4 2019.

[7] L. Gupta, R. Jain, and G. Vaszkun, "Survey of important issues in uav communication networks," IEEE Communications Surveys Tutorials, vol. 18, pp. 1123–1152, 2016.

[8] J. Lyu, Y. Zeng, R. Zhang, and T. J. Lim, "Placement optimization of uav-mounted mobile base stations," IEEE Communications Letters, vol. 21, pp. 604–607, 3 2017.

[9] U. Challita, W. Saad, and C. Bettstetter, "Interference management for cellular-connected uavs: A deep reinforcement learning approach," IEEE Transactions on Wireless Communications, vol. 18, pp. 2125–2140, 4 2019.

[10] Y. Zeng, J. Lyu, and R. Zhang, "Cellular-connected uav: Potential, challenges, and promising technologies," IEEE Wireless Communications, vol. 26, pp. 120–127, 2 2019.

[11] G. Virone, F. Paonessa, L. Ciorba, M. Lumia, G. Addamo, O. A. Peverini, and P. Bolli, "Effect of conductive propellers on vhf uav-based antenna measurements: Experimental results." IEEE, 2021 IEEE Conference on Antenna Measurements & Applications (CAMA), 15-17 November 2021, Antibes Juan-les-Pins, France11 2021, pp. 46–47.